

Article

Capacitive Imaging for Skin Characterizations and Solvent Penetration Measurements

Xu Zhang ^{1,2}, Christos Bontozoglou ² , Elena Chirikhina ², Majella E. Lane ³ and Perry Xiao ^{2,*} 

¹ Auckland Tongji Medical & Rehabilitation Equipment Research Center, Tongji Zhejiang College, No. 168 Business Road, Zhejiang 314051, China; zhangx12@lsbu.ac.uk

² School of Engineering, London South Bank University, 103 Borough Road, London SE1 0AA, UK; cbontoz@gmail.com (C.B.); info@sinlen.co.uk (E.C.)

³ UCL School of Pharmacy, 29–39 Brunswick Square, London WC1N 1AX, UK; majella.lane@btinternet.com

* Correspondence: xiaop@lsbu.ac.uk; Tel.: +44-20-7815-7569; Fax: +44-20-7815-7561

Received: 2 July 2018; Accepted: 28 August 2018; Published: 1 September 2018



Abstract: Capacitive contact imaging has shown potential in measuring skin properties including hydration, micro relief analysis, as well as solvent penetration measurements. Through calibration, we can also measure the absolute permittivity of the skin, and from absolute permittivity we then work out the absolute water content and absolute solvent content in skin. This paper presents our latest study of capacitive contact imaging for skin characterizations and vivo skin solvent penetration. The results show that with capacitive contact imaging, it is possible not only to assess the skin damaging, but also potentially possible to differentiate different types of skin damages. The results also show that with capacitive contact imaging, it is also possible to measure the solvent penetration through skin and to quantify the solvent concentration within skin.

Keywords: capacitive imaging; skin hydration; solvent penetration; water content; solvent content

1. Introduction

Skin characterization, such as skin damage assessments, and skin solvent penetrations are important for many skin clinical trial studies. However, measuring and quantifying skin damage are not easy. Recent studies include using transepidermal water loss (TEWL) and skin conductance to test the skin barrier integrity [1], and using Tissue Viability Imaging to detect venous stasis in the skin [2]. To measure and quantify solvent penetration through the skin are even more difficult. Microdialysis is a commonly used technique [3]. It is label-free and can be used to continuously monitor drug concentrations in the extracellular fluid of tissue. But it is not non-invasive. Stimulated Raman scattering (SRS) is another recently-developed label-free chemical imaging technique [4], but it is expensive and can only work on in-vitro samples. There is a genuine need for a simple, accurate technique for skin damage assessments and skin solvent penetrations.

Capacitive contact imaging, originally designed by biometric applications (i.e., fingerprints) has shown potentials in skin hydration imaging, skin texture analysis, and skin solvent penetration measurements [5–10]. It is based on capacitance measurement principles, and the measurement results depend on the sample's dielectric permittivity. Through calibration, we can get the absolute dielectric permittivity of the sample. This is different from other similar devices on the market, which are uncalibrated. Our latest studies showed that capacitive contact imaging can also be used for many solvents, due to their relative high dielectric permittivity comparing with skin [11,12]. This makes the technique very useful for in-vivo trans-dermal drug delivery studies. The aim of this study is to evaluate the performance of using capacitive imaging for skin characterization, i.e., skin damage assessments, as well as to quantitatively measure the in-vivo skin solvent penetrations.

2. Materials and Methods

2.1. Epsilon Permittivity Imaging System

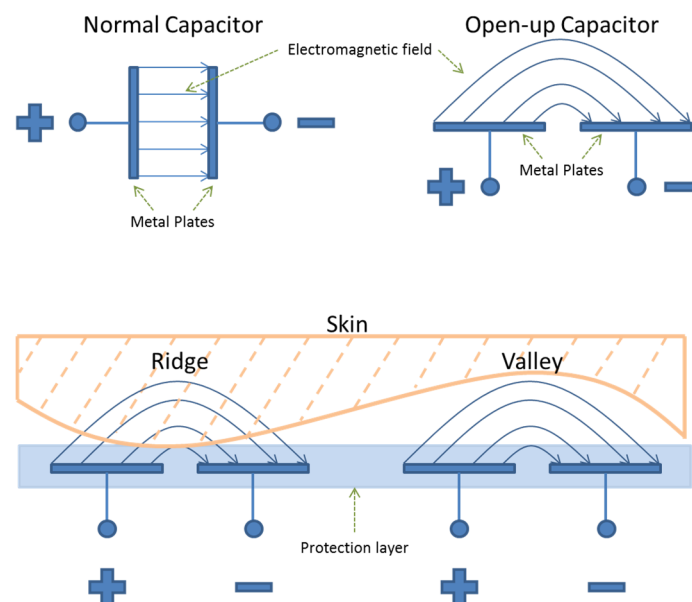
In this study, capacitive contact imaging is achieved by using the Epsilon permittivity imaging system (Biox Systems Ltd., London, UK). The Epsilon permittivity imaging system is based on Fujitsu fingerprint sensors (Fujitsu Ltd., Tokyo, Japan) and has 256×300 pixels with $50 \mu\text{m}$ spatial resolution, as shown in Figure 1 [12]. Each pixel is equivalent of a capacitive sensor, which measures the dielectric constant or permittivity of the sample. Epsilon has an 8-bit grey-scale capacitance resolution per pixel (0–255).



(a) Epsilon and the in-vivo stand.



(b) Epsilon and the in-vitro stand.



(c) Capacitive fingerprint sensor measurement principle.

Figure 1. Epsilon Permittivity Imaging System: (a) Epsilon and the in-vivo stand; (b) Epsilon and the in-vitro stand; (c) its measurement principle.

2.2. Epsilon Calibration

Unlike other similar skin measurement instruments on the market, Epsilon is fully calibrated, which means it has a linear response to sample's near-surface dielectric permittivity, see Figure 2. Calibration is done by measuring the dielectric constants of a list of materials with well know dielectric constants, such as dry air, propanol, glycerol and distilled water etc. The linear response is important because hydration is linearly related to permittivity. The calibration ensures consistency from instrument to instrument and from time to time. With calibrated Epsilon imaging systems, we can measure the absolute dielectric permittivity of the material. A RGB colour scheme is used to represent the dielectric constant values, the brighter the colour, the higher the dielectric constant, and darker the colour, the lower the dielectric constant.

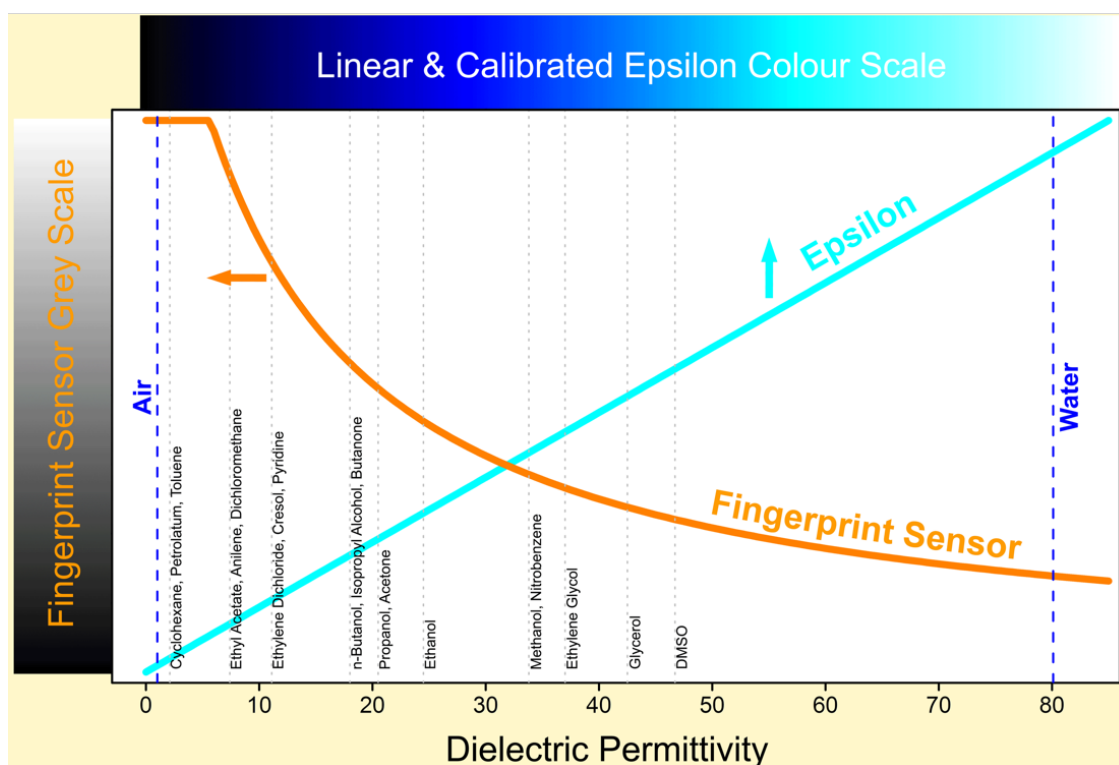


Figure 2. The Epsilon calibration curve and linear response to dielectric permittivity.

2.3. Skin Hydration and Solvent Concentration Calculations

If we assume measured skin dielectric constant value (ϵ_m) is linearly dependent on that of dry skin (ϵ_{dry}) and water (ϵ_{water}), i.e.,

$$\epsilon_m = \epsilon_{dry} \times \left(1 - \frac{H}{100}\right) + \epsilon_{water} \times \frac{H}{100} \quad (1)$$

where H is water concentration in skin as percentage of volume ratio, then we can work out the water content using following equation [6]:

$$H = \frac{\epsilon_m - \epsilon_{dry}}{\epsilon_{water} - \epsilon_{dry}} \times 100 \quad (2)$$

For the solvent penetration through skin, measured dielectric constant value (ϵ_m) is a combination of pure solvent (ϵ_{sol}) and skin (ϵ_{skin}), similar to Equation (2), we also can calculate the solvent concentration (C , volume ratio percentage),

$$C = \frac{\varepsilon_m - \varepsilon_{skin}}{\varepsilon_{sol} - \varepsilon_{skin}} \times 100 \quad (3)$$

In the paper, the dielectric constants we used for water is $\varepsilon_{water} = 80.1$, for dry skin is $\varepsilon_{dry} = 1$, for pure alcohol is $\varepsilon_{sol} = 24.3$, for pure ethylene glycol is $\varepsilon_{sol} = 55.81$, and for pure glycerol is $\varepsilon_{sol} = 38.91$.

2.4. Re-Positioning Using Normalized Cross-Correlation Algorithm

Re-positioning is very important in image processing. During many occasions, we would prefer to compare the results from exactly the same skin area. To select the same skin area manually is cumbersome and inaccurate. We have developed an efficient repositioning technique based on normalized cross-correlation algorithm. As illustrated in Figure 3, users can select the region of interests (RoI) in the first image, the re-positioning technique will automatically find the exactly same position in the subsequent images.

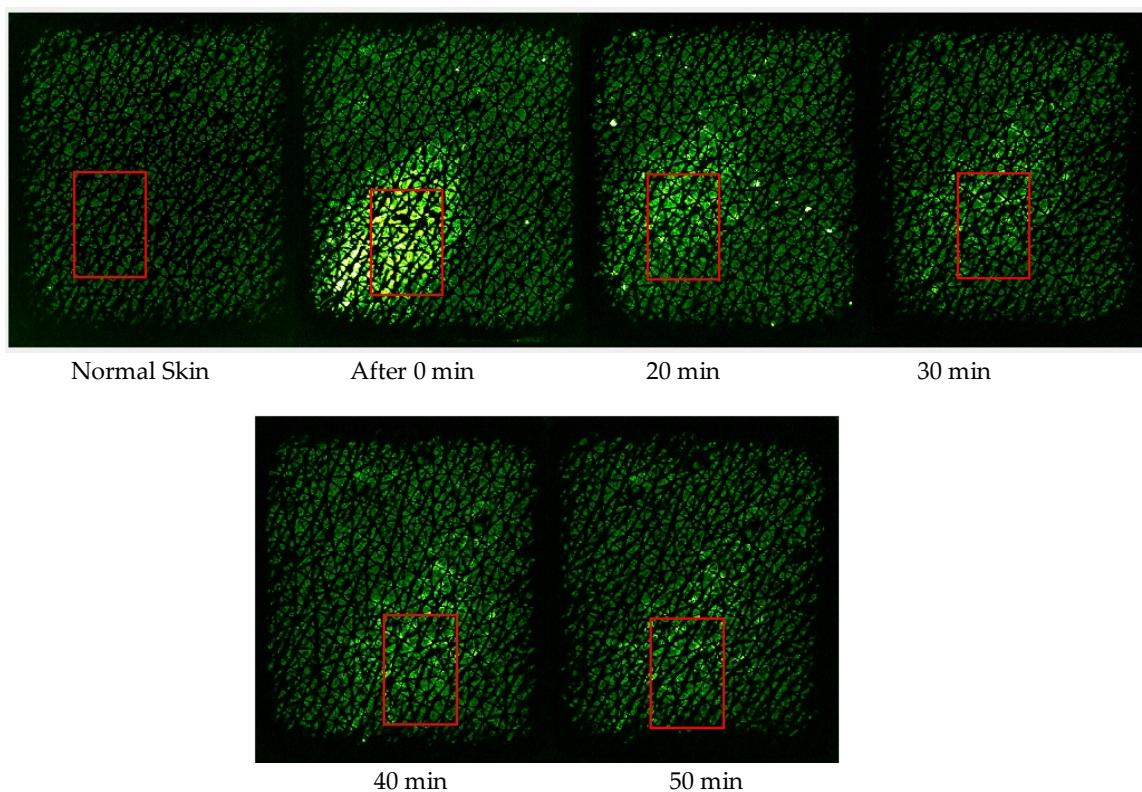


Figure 3. Capacitive contact images of skin before and after Glycerol application. Red squares show the repositioning of the RoI in Normal Skin image (before application) and in the consequent images (after application).

If we use matrix R to represent the region of interests, and matrix T to represent the target images, we first normalized the R using following formula,

$$R_N = \frac{R - \min}{\max - \min} \times 255 \quad (4)$$

where \max and \min are the maximum value and minimum value of R , and R_N is the normalized R . Similarly we can also normalize T to get R . Then we can calculate the cross-correlation of R_N and T_N as,

$$Corr = \sum_i \left(\frac{\sum_j (R_N(j) - RM) \times (T_N(j - i) - TM)}{\sqrt{\sum_j (R_N(j) - RM)^2} \times \sqrt{\sum_j (T_N(j - 1) - TM)^2}} \right) \quad (5)$$

where i and j are the matrix indexes, RM is the mean of R_N and TM is the mean of T_N . From calculation result $Corr$, we can find out at which position that two matrices are best correlated, and that will be the position of the original region of interests R in target image T .

2.5. Experimental Procedures

All the measurements were performed by using the calibrated Epsilon permittivity imaging system, which was placed on the test skin area for a period of one minute, skin capacitance images were recorded continuously. Re-positioning algorithm is used when analysing the images, to make sure all the results are from exactly the same skin area. The laboratory conditions are 21 ± 1 °C and $45 \pm 5\%$ RH. The volar forearm skin sites from two healthy volunteers (aged 20–40) were chosen for this study. The volunteers were acclimatized in the laboratory for 20 min prior to the experiments.

For skin characterization, three types of skin damages were studied: intensive washes, tape stripping and sodium lauryl sulphate (SLS) irritation. For intensive washes, room temperature running water and washing-up liquid (Fairy, P&G, Weybridge, UK) were used to rub the skin site gently for 3 min with a finger. After wash, the skin site was carefully patted dry with a tissue before the measurements. Tape stripping was performed 20 times per site by the use of standard clear 3 M Scotch sellotape (25×66 mm²). SLS irritation was achieved by applying 2% SLS water solution (v/v , volume ratio) on skin. SLS is a commonly used detergent and surfactant in soaps, shampoos and toothpaste etc. SLS can help to remove dirt and grease from the skin. But SLS residue left on skin surface can cause skin dryness and irritation [13]. Capacitive contact imaging measurements were performed both before and after. The measurements were done by using capacitive imaging sensor to occlude the skin test sites for a period of one minute, during which skin capacitance images were recorded continuously at the rate of one image per second. The reason to occlude the skin for one minute is to investigate how the occlusion curves change during the skin damage. The average water contents of the images were then calculated at different times during occlusion using Equation (2).

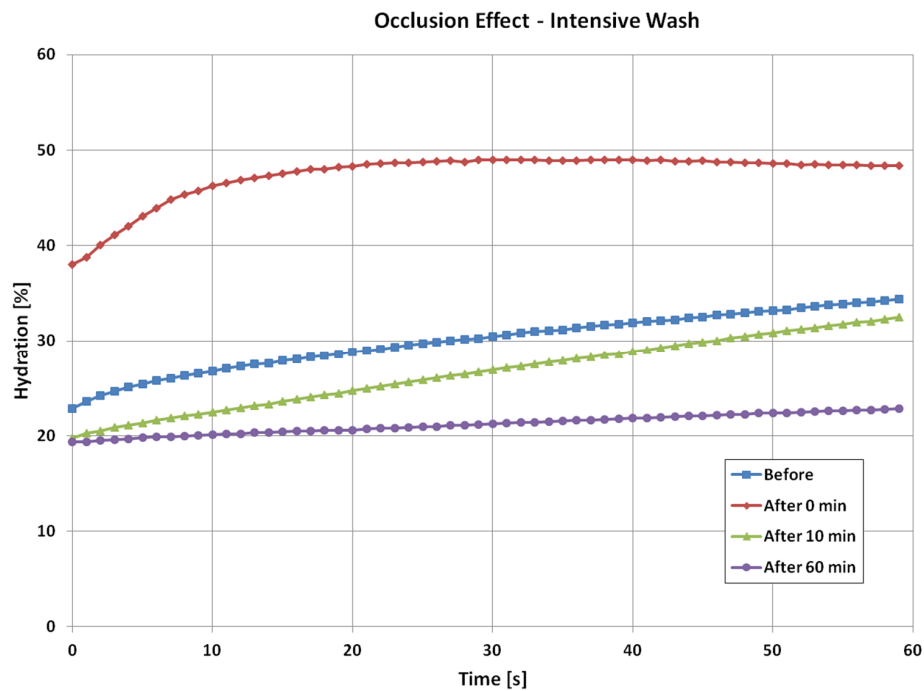
For skin solvent penetration measurements, three solvents were studied, pure ethanol, pure ethylene glycol, and pure glycerol. A small quantity of solvent (a few millilitres), held in a plastic well, was applied on skin site for 5 min the skin site was then carefully wiped clean to make sure no solvent residue left on skin surface. The capacitive imaging measurements were performed both before and after the application. Again, the measurements were done by using capacitive imaging sensor to occlude the skin test sites for a period of one minute, during which skin capacitance images were recorded continuously at the rate of one image per second. The solvent concentrations in skin were calculated by using Equation (4), and the re-positioning technique was used to make sure the calculations are done on exactly the same skin site.

3. Experimental Results

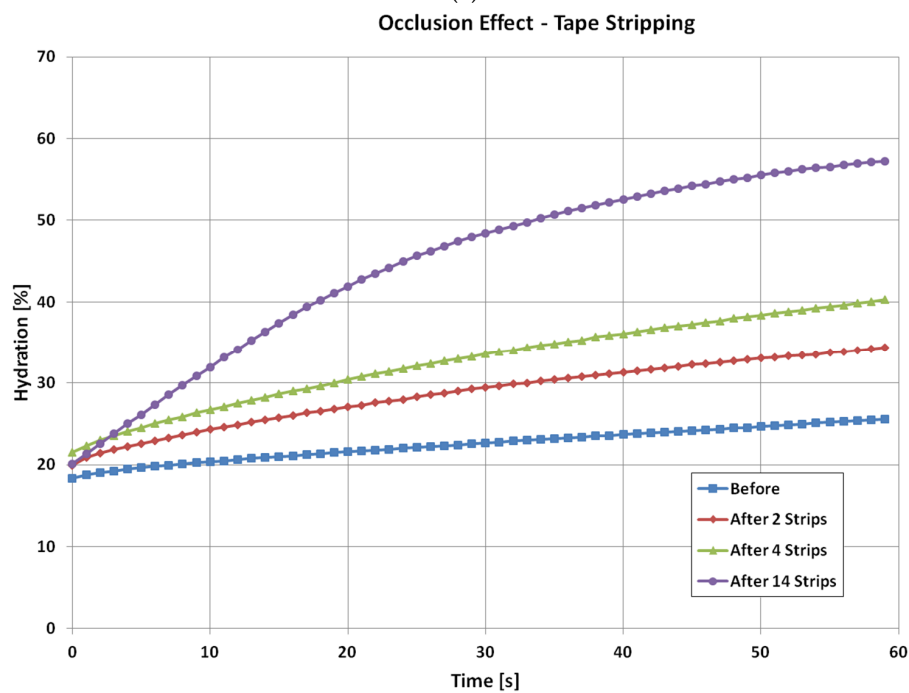
3.1. Skin Damage Characterizations

Figure 4 shows the time dependent skin hydration occlusion curves over the period of one minute, before and after the intensive wash, tape stripping and SLS irritation. For the intensive wash, the occlusion curve before the washes, i.e., normal skin, is relatively low, and less curved. Immediately after the wash, the occlusion curve is high and more curved. This is because skin is hydrated after the wash, and also some skin surface layers were removed during the washing, which caused the curvature of the occlusion curve to change. Then, as skin recovers under ambient condition, the occlusion curves gradually returns to its normal value and shape. After 10 min of the intensive, the occlusion curve start to go below the original normal skin level, and after 60 min it goes even lower. This is the drying effect of intensive wash, as the washing liquid has removed dirt, sweat sebum, and oils etc., from skin surface by using surfactants, which surround dirt and oil, dissolving them and making it easier for water to wash them away. This hence caused the skin to become drier [14].

For the tape stripping, the occlusion curve before the tape stripping is again relatively low and less curved. Immediately after the two tape stripping, the starting value of the occlusion curve is similar, only slightly increases, but the curvature of the curve starts to change more, this is because tape stripping has removed many layers of skin and cause the skin structure to change. As the tape stripping goes on, the curvature changes become more and more significant. After 14 tape strips, the occlusion curve is significantly different from that of initial normal skin.



(a)



(b)

Figure 4. Cont.

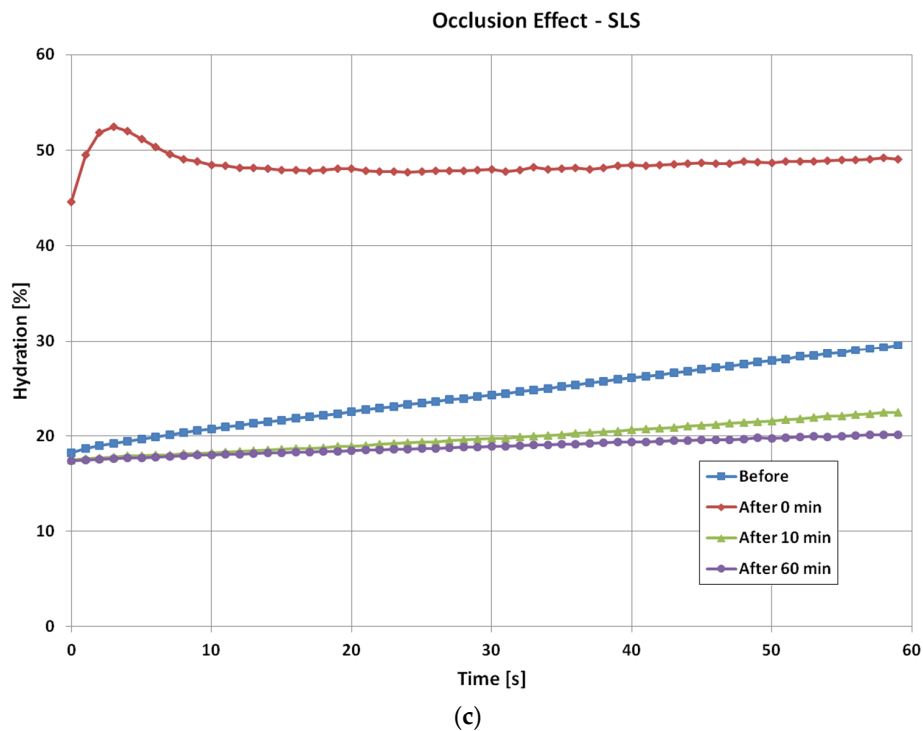


Figure 4. The time dependent skin hydration occlusion curves before and after the intensive wash (a); tape stripping (b); SLS irritation (c).

For the SLS irritation, the occlusion curve before the tape stripping is similar to previous two cases. However, immediately after the SLS irritation, the occlusion curve becomes very high. This is because the SLS water solution also hydrated the skin. The initial hump in the occlusion curve is due to image processing, it is not a skin feature. Then as skin recovers, the occlusion curve returns to its normal level. Similar to the intensive wash results, after 10 min the occlusion curve starts to go below that of the original normal skin, and stays at the similar level even after 60 min. This is also the skin drying effect, as SLS removes skin surface dirt and grease, which caused skin to become drier.

Figure 5 shows corresponding capacitive contact images at the half way (time = 30 s) of the one minute occlusion measurements, before and after intensive washes, tape stripping and SLS irritation measurements. The skin images are generally getting brighter after damage, which indicates higher water content in skin. In both intensive washes and SLS irritation, the darker recovery skin images, starting from 10 min after, indicate there is a drying effect after the damage.

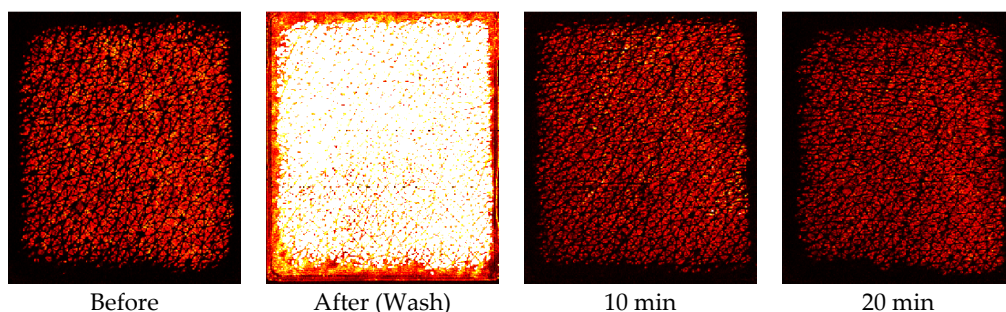


Figure 5. Cont.

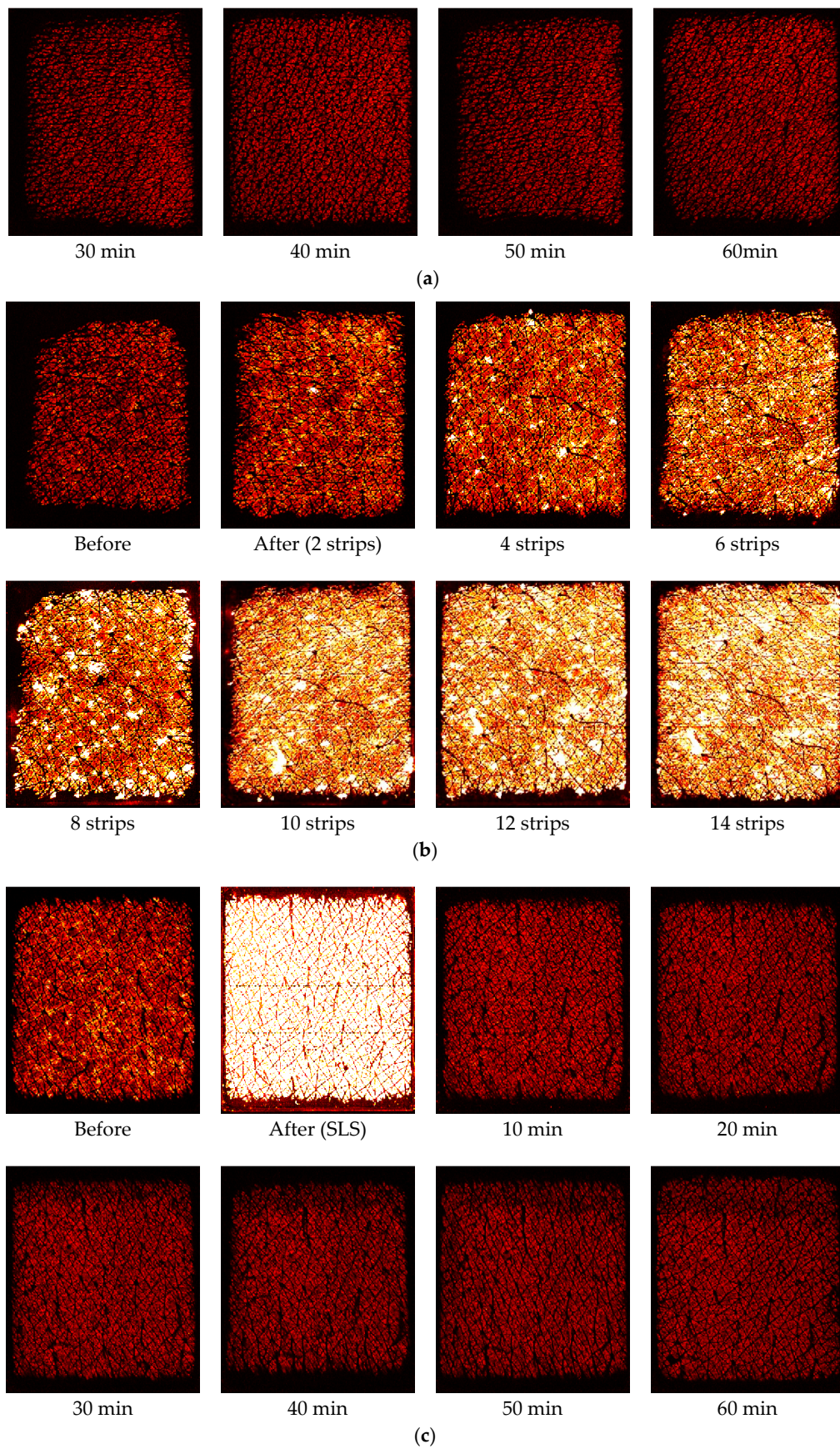


Figure 5. Typical capacitive contact images of before and after intensive washes (a); tape stripping (b); SLS irritation (c).

3.2. Skin Solvent Penetrations

Figure 6 shows the capacitive images at the half way (time = 30 s) of the one minute occlusion measurements, before and after the three solvent applications. The darker ring in the images after the solvent application is caused by the plastic well, as pressure was applied to the plastic well, to make sure the solvents are not to leak outside the well. Therefore, the area within the darker ring reflects more of the solvents, and the area outside the darker ring reflects more of the skin. The slight brightness just outside the darker rings, particularly for Ethylene Glycol, is likely due to the solvent lateral diffusion underneath the skin.

The next step is to quantify the solvent concentration in skin. Figure 7 shows the corresponding calculated solvent concentration (volume ratio percentage, v/v) from the images shown in Figure 6 as volume ratio percentages before after solvent applications using Equation (3). The solvent concentration is set to zero before the application. The calculated results agree well with the image results, i.e., Ethylene Glycol can penetrate into skin the most, and can also disappearing into deeper skin quicker, Ethanol can penetrate into skin the least, whilst Glycerol is somewhere in the middle, and stays in the skin longer.

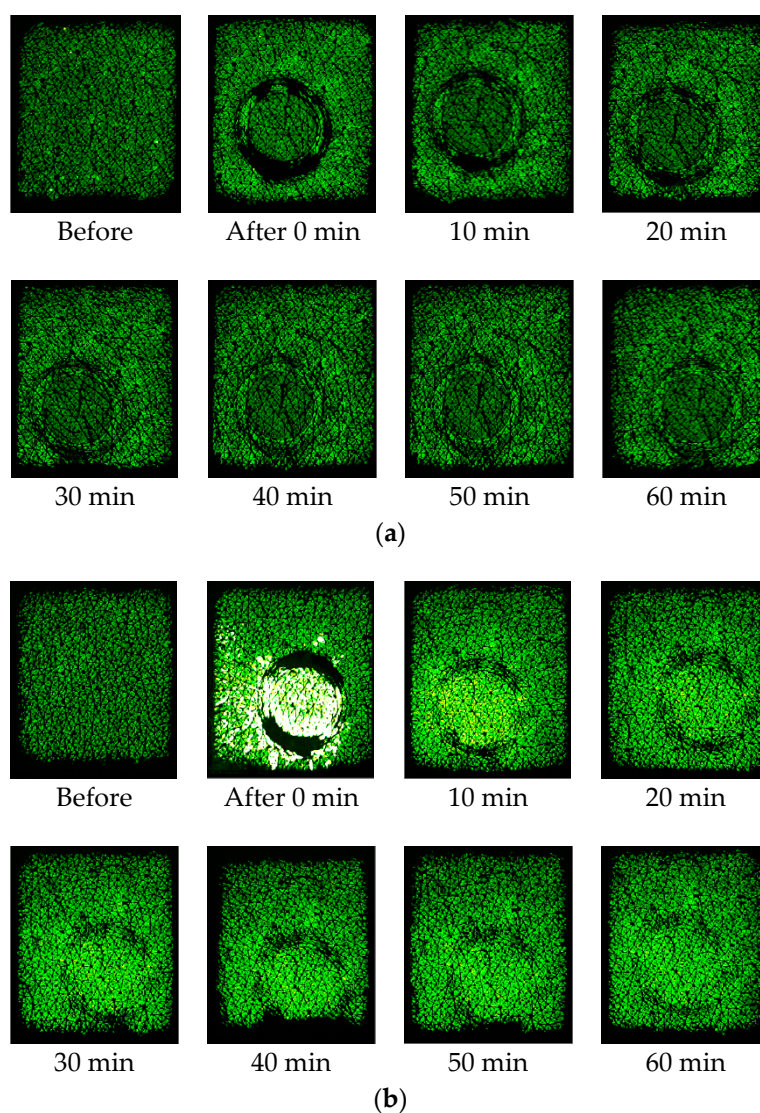


Figure 6. Cont.

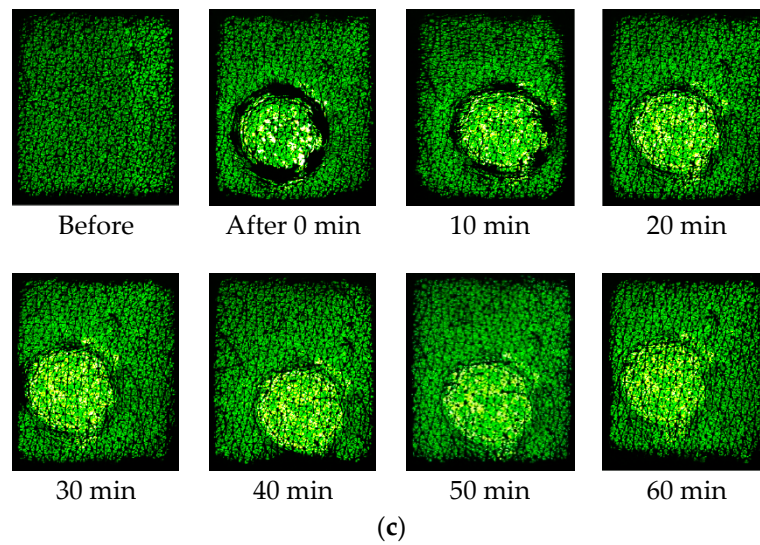


Figure 6. Capacitive contact images of skin before and after solvent applications, (a) Ethanol; (b) Ethylene Glycol; (c) Glycerol.

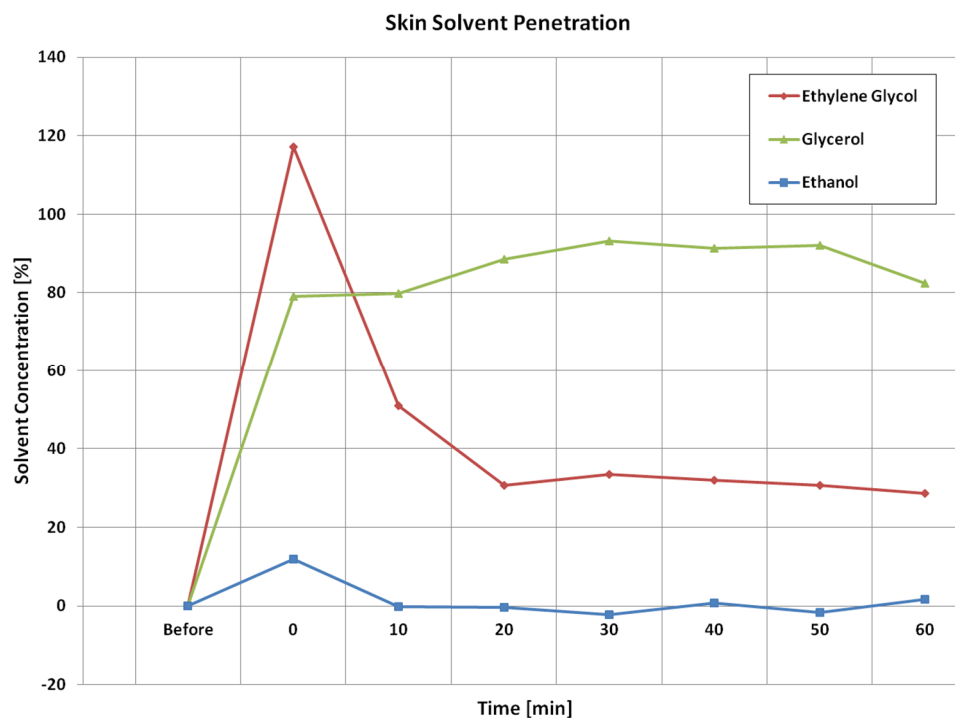


Figure 7. The calculated solvent concentration as volume ratio percentage before after solvent applications.

4. Discussions

For three types of skin damage experiments, i.e., intensive washes, tape stripping and sodium lauryl sulphate (SLS) irritation, the results show that the levels of occlusion curves reflect the hydration levels of the skin. For normal skin, it is low, and when skin is damaged, i.e., by washing, tape stripping, and SLS irritation, it becomes high. The shapes of occlusion curves, i.e., the curvature, reflect the skin structure, when skin is damaged, and the curvature of the curves changes. Therefore, from the levels and the shapes we can understand how much the skin is damaged, and how long does it take to recover. It also is interesting to point out that for different types of skin damages, the time dependent occlusion

curves are also different. This suggests that it is possible to use these time dependent occlusion curves to characterize skin, i.e., not only to show how much the skin is damaged, but also to show what types of damages. In both intensive washes and SLS irritation, an obvious drying effect was observed after the damage.

For the skin solvent penetration experiment, i.e., Ethanol, Ethylene Glycol, and Glycerol, the image results show that after 5 min application, Ethylene Glycol penetrates most into the skin, while Ethanol penetrates the least. This is understandable, as Ethanol is very volatile, and evaporated quickly after the application. Ethylene Glycol also disappears quicker from the skin surface. As Ethylene Glycol is non-volatile, we assume it goes into deeper skin. Glycerol, however, tends to stuck within the skin for a long period of time. The calculated solvent concentration results show that Ethylene Glycol has the highest increase after the application, this means Ethylene Glycol can penetrate more into the skin. Then, as time goes on, the Ethylene Glycol concentration starts to reduce, the fast reduction rate shows that Ethylene Glycol can penetrate skin from surface into deep skin site very easily. There is an overshoot (>100%) in Ethylene Glycol concentration, which is likely due to the increase of skin water content, as during the 5 min solvent application, skin water content is likely to increase due to solvents blocking the water loss. So for the further work, next step is to develop a new method that can eliminate the effect of water is solvent concentration calculation. Glycerol concentration in skin reaches the second highest level after the application. Also, the Glycerol concentration stays more or less the same for about 60 min period of time, this indicates that Glycerol is not penetrating through skin easily, it is more likely to get stuck within the skin. The Ethanol concentration has the smallest increase. This is because Ethanol is highly volatile. The slight negative undershoots in Ethanol results are likely due to the skin drying because of Ethanol application.

The advantages of capacitive contact imaging is it can produce an image of water and solvent content in skin, and it is simple and quick to use. The disadvantages are it is a contact technology, it cannot differentiate different types of solvents, and it has limited penetration depths of about 20–50 microns.

5. Conclusions

We presented our study on capacitive contact imaging for skin characterization and skin solvent penetration measurements. Unlike other technologies, our capacitive contact imaging is fully calibrated, which means we can measure the absolute dielectric properties of the skin, and from which we can quantify the absolute skin water content, as well as the absolute solvent concentrations in skin. We have also developed an effective skin re-positioning technique, to ensure that we analyze the same skin area for all the measurements, this will increase the accuracy and repeatability of results.

The results show that capacitive contact imaging can effectively characterize the skin damages. Using the time dependent occlusion curves, it is possible to not only show how much the skin is damaged, but also how it is damaged, i.e., by intensive washes, or by tape stripping, or by SLS irritation, as different types of damages will result in different types of occlusion curves. The skin solvent penetration results show that capacitive contact imaging can differentiate different types of solvent and, mostly importantly, quantify the amount of the solvent absorbed by skin.

Author Contributions: Conceptualization, X.Z., C.B. and P.X.; Methodology, X.Z. and P.X.; Software, C.B.; Validation, X.Z., C.B. and P.X.; Formal Analysis, X.Z. and C.B.; Investigation, X.Z. and E.C.; Resources, M.E.L.; Data Curation, X.Z.; Writing-Original Draft Preparation, X.Z.; Writing-Review & Editing, X.Z., M.E.L. and P.X.; Visualization, X.Z. and E.C.; Supervision, P.X.; Project Administration, P.X.; Funding Acquisition, P.X.

Funding: This research received no external funding.

Acknowledgments: We thank London South Bank University for the financial support, we also thank Biox Systems Ltd for sponsoring the PhD studentship of CB.

Conflicts of Interest: The authors declare no conflict of interest.

References

1. Zhang, Q.; Murawsky, M.; LaCount, T.; Kasting, G.B.; Li, S. Transepidermal water loss and skin conductance as barrier integrity tests. *Toxicol. In Vitro* **2018**, *51*, 129–135. [[CrossRef](#)] [[PubMed](#)]
2. Bergqvist, M.; Henricson, J.; Iredahl, F.; Tesselaar, E.; Sjöberg, F.; Farnebo, S. Assessment of microcirculation of the skin using Tissue Viability Imaging: A promising technique for detecting venous stasis in the skin. *Microvasc. Res.* **2015**, *101*, 20–25. [[CrossRef](#)] [[PubMed](#)]
3. Marchand, S.; Chauzy, A.; Dahyot-Fizelier, C.; Couet, W. Microdialysis as a way to measure antibiotics concentration in tissues. *Pharm. Res.* **2016**, *111*, 201–207. [[CrossRef](#)] [[PubMed](#)]
4. Saar, B.G.; Contreras-Rojas, L.R.; Xie, X.S.; Guy, R.H. Imaging drug delivery to skin with stimulated Raman scattering microscopy. *Mol. Pharm.* **2011**, *8*, 969–975. [[CrossRef](#)] [[PubMed](#)]
5. Léveque, J.L.; Querleux, B. SkinChip, a new tool for investigating the skin surface in vivo. *Skin Res. Technol.* **2003**, *9*, 343–347. [[CrossRef](#)] [[PubMed](#)]
6. Batisse, D.; Giron, F.; Léveque, J.L. Capacitance imaging of the skin surface. *Skin Res. Technol.* **2006**, *12*, 99–104. [[CrossRef](#)] [[PubMed](#)]
7. Xiao, P.; Singh, H.; Zheng, X.; Berg, E.P.; Imhof, R.E. In-vivo Skin Imaging for Hydration and Micro Relief Measurements. In Proceedings of the Stratum Corneum V Conference, Cardiff, UK, 11–13 July 2007.
8. Bevilacqua, A.; Gherardi, A. Characterization of a capacitive imaging system for skin surface analysis. In Proceedings of the First Workshops on Image Processing Theory, Tools and Applications, Sousse, Tunisia, 9 January 2009. [[CrossRef](#)]
9. Singh, H.; Xiao, P.; Berg, E.P.; Imhof, R.E. Skin Capacitance Imaging for Surface Profiles and Dynamic Water Concentration Measurements. In Proceedings of the ISBS Conference, Seoul, Korea, 7–10 May 2008.
10. Ou, X.; Pan, W.; Xiao, P. In vivo skin capacitive imaging analysis by using grey level co-occurrence matrix (GLCM). *Int. J. Pharm* **2014**, *460*, 28–32. [[CrossRef](#)] [[PubMed](#)]
11. Xiao, P.; Lane, M.E.; Abdalghafor, H.M. Membrane Solvent Penetration Measurements Using Contact Imaging. In Proceedings of the Stratum Corneum VII Conference, Cardiff, UK, 10–12 September 2012.
12. Xiao, P.; Ou, P.; Ciordea, L.I.; Berg, E.P.; Imhof, R.E. In-vivo skin solvent penetration measurements using opto-thermal radiometry and fingerprint sensor. *Int. J. Thermophys.* **2012**, *33*, 1787–1794. [[CrossRef](#)]
13. Danby, S.G.; Brown, K.; Wigley, A.M.; Chittock, J.; Pyae, P.K.; Flohr, C.; Cork, M.J. The effect of water hardness on surfactant deposition after washing and subsequent skin irritation in atopic dermatitis patients and healthy control subjects. *J. Investig. Dermatol.* **2018**, *138*, 68–77. [[CrossRef](#)] [[PubMed](#)]
14. Seweryn, A. Interactions between surfactants and the skin—Theory and practice. *Adv. Colloid Interface Sci.* **2018**, *256*, 242–255. [[CrossRef](#)] [[PubMed](#)]



© 2018 by the authors. Licensee MDPI, Basel, Switzerland. This article is an open access article distributed under the terms and conditions of the Creative Commons Attribution (CC BY) license (<http://creativecommons.org/licenses/by/4.0/>).